

## RESEARCH AND EDUCATION

## Effect of industrial scanner and framework material interaction on the marginal gaps of CAD-CAM complete-arch implant frameworks

Burak Yilmaz, DDS, PhD,<sup>a</sup> Xiaohan Guo, BSc,<sup>b</sup> Martin Schimmel, Prof Dr med dent,<sup>c</sup> and Samir Abou-Ayash, PD Dr med dent<sup>d</sup>

### ABSTRACT

**Statement of problem.** Structured-light and computed tomography industrial scanners have been used as reference scanners to measure marginal gaps between implants and superstructures. However, the effect of framework material on the scanners' ability to detect gaps and on precision has not yet been evaluated.

**Purpose.** The purpose of this in vitro study was to investigate the interaction between the industrial scanner and framework material on measured marginal gaps of implant-supported fixed complete-arch frameworks made from titanium and polymethylmethacrylate and on the precision of scans.

**Material and methods.** A completely edentulous maxillary model with 4 implants and multiunit abutments at the first molar and canine sites was digitized by using a laboratory scanner. Implant-supported frameworks were milled from titanium and polymethylmethacrylate ( $n=5$ ). Each framework was secured on the left molar site abutment. The marginal gaps between the frameworks and abutment sites without a screw were measured by using an industrial structured-light scanner and an industrial computed tomography scanner. The effect of the scanner, the framework material, and their interaction on measured gaps was analyzed by applying linear regressions and weighted least square methods. The F-statistics was used with Bonferroni corrections for precision analysis ( $\alpha=.05$ ).

**Results.** No significant effect of scanner, material, or their interaction was found on the marginal gaps at the canine sites. The titanium framework gaps detected by using the computed tomography scanner were greater than those detected by using the structured-light scanner at the right molar site (estimated difference in means=0.054 mm;  $P=.003$ ) and overall (estimated difference in means=0.023 mm;  $P=.033$ ). The structured-light scanner's precision was higher than that of the computed tomography scanner when titanium frameworks were scanned ( $P=.001$ ). The computed tomography scanner's precision was higher when scanning polymethylmethacrylate frameworks than when scanning titanium frameworks ( $P=.03$ ).

**Conclusions.** Framework material and industrial scanner interaction affected the measured gaps. The computed tomography scanner detected greater marginal gaps with low precision when scanning titanium frameworks than the structured-light scanner. The sample size, the use of only 2 types of materials, and a laboratory scanner to obtain the computer-aided design file should be considered when interpreting the results. (*J Prosthet Dent* 2021;■■:■■-■■)

An accurately fitting implant-supported complete-arch prosthesis is essential, as ill-fitting frameworks may lead to complications.<sup>1-7</sup> However, measuring marginal gaps

can be challenging because of the bulk of the frameworks, which may prevent the marginal gaps being detected, particularly when they are located

<sup>a</sup>Associate Professor, Department of Reconstructive Dentistry and Gerodontology, School of Dental Medicine, University of Bern, Bern, Switzerland; and Associate Professor, Department of Restorative, Preventive and Pediatric Dentistry, School of Dental Medicine, University of Bern, Bern, Switzerland; and Adjunct Professor, Division of Restorative and Prosthetic Dentistry, The Ohio State University College of Dentistry, Columbus, Ohio.

<sup>b</sup>PhD student, Division of Biostatistics, College of Public Health, The Ohio State University, Columbus, Ohio.

<sup>c</sup>Department Head, Department of Reconstructive Dentistry and Gerodontology, University of Bern, Bern, Switzerland; and Senior Lecturer, Extra muros, Division of Gerodontology and Removable Prosthodontics, University Clinics of Dental Medicine, University of Geneva, Geneva, Switzerland.

<sup>d</sup>Senior Lecturer and Head of the Section of Digital Implant and Reconstructive Dentistry, Department of Reconstructive Dentistry and Gerodontology, University of Bern, Bern, Switzerland.

## Clinical Implications

An industrial structured-light scanner may be preferred to an industrial computed tomography scanner for the evaluation of gaps at titanium-titanium interfaces because of its higher precision. Both scanners may be used to evaluate the marginal gaps of polymethylmethacrylate frameworks. Even though the tested scan techniques are not applicable for intraoral use, they may be used by implant manufacturers or dental laboratory technicians for quality control.

subgingivally.<sup>8</sup> The vertical and horizontal gaps at the margin and the internal gaps between the mating surfaces have been commonly measured by using 2-dimensional methods.<sup>2</sup> With the advent of digital technology, the 3-dimensional (3D) digital measurement of marginal gaps has become possible with different imaging systems.<sup>3,7,9-11</sup> The triple-scan technique, which is based on optical or tactile scans, has been used to evaluate the marginal gaps of single- and multiple-unit restorations,<sup>7,9-11</sup> commonly in combination with a best-fit algorithm. This algorithm attempts to find the superimposition of 2 surface scans with the minimum difference between all surface points.<sup>12</sup> However, the authors are unaware of studies that have used the triple-scan technique for implant-supported complete-arch frameworks. Also, highly reflective or translucent materials may require coating when structured-light scanners are used because their surfaces may become a source of measurement error in addition to system-related measurement inaccuracies.<sup>7,13</sup> Therefore, the surface properties and the density of the material scanned may influence the scan accuracy.<sup>14</sup>

An industrial metrology-grade computed tomography (CT) scanner has been used to scan frameworks and measure the marginal gap *in vitro*,<sup>3-5</sup> with a different working mechanism compared with structured-light scanners with the triple-scan technique. Industrial CT scanners can capture the interfaces with 1 scan, without the need to scan and stitch objects together.<sup>3-5</sup>

Both industrial structured-light and CT scanners have been used as reference scanners by researchers,<sup>2</sup> and different digital methods to evaluate marginal gaps with implant frameworks have been reported.<sup>2</sup> However, whether these industrial scanner scans are comparable is not clear, and the authors are unaware of studies comparing the ability of industrial scanners with varying mechanisms to detect marginal gaps of complete-arch implant frameworks in different materials.

The aim of the present study was to investigate the industrial scanner (structured-light or CT) and

framework material interaction on the measured marginal gaps of implant-supported fixed complete-arch computer-aided design and computer-aided manufacturing (CAD-CAM) titanium (Ti) and polymethylmethacrylate (PMMA) frameworks. The null hypotheses were that the measured marginal gaps of frameworks at different abutment sites and overall would not be affected by scanner-material interaction, that the precision of the scans would not be different, and that they would not be affected by the framework material.

## MATERIAL AND METHODS

The present study followed the methodology of previous studies.<sup>3-5</sup> A screw-retained complete-arch acrylic resin (Pattern Resin LS; GC America Inc) prototype with abutment-level titanium copings (Temporary Snap Coping Multi-unit Plus; Nobel Biocare AG) fitted on conical multiunit abutments was fabricated on a maxillary typodont model with 2 straight implants parallel to each other (Nobel Active RP 4.3×13 mm; Nobel Biocare AG) in the anterior region and 2 implants (Nobel Active RP 4.3×13 mm; Nobel Biocare AG) with a 30-degree distal tilt in the posterior region. Straight abutments (Multi-unit Abutment Plus Conical Connection RP 2.5 mm; Nobel Biocare AG) were attached to the anterior implants, and 30-degree angulated abutments (30° Multi-unit Abutment Plus Conical Connection RP 3.5 mm; Nobel Biocare AG) to the posterior implants. The framework was sectioned and reconnected with the same acrylic resin to compensate for polymerization shrinkage. A 3D laboratory scanner (S600 ARTI; Zirkonzahn GmbH) with the manufacturer's specified measuring inaccuracy of  $\leq 10 \mu\text{m}$  was used to digitize the model with titanium scan bodies (Nobel Biocare Scanmarker NP-RP; Zirkonzahn GmbH), and the resin prototype was tightened to 15 Ncm on each of the 4 screw-retained abutments to generate an accurately fitting virtual 3D CAD (Zirkonzahn.Modellier; Zirkonzahn GmbH) framework in a standard tessellation language (STL) file. A 5-axis +1 milling unit (M1 Wet Heavy Metal Milling Unit; Zirkonzahn GmbH) was used to mill 5 frameworks from PMMA (Temp Premium A1-B1-95H16; Zirkonzahn GmbH) and Ti (Titan 5-95H14; Zirkonzahn GmbH) according to the manufacturer's instructions.

The frameworks were placed on the typodont model, and the 1-screw test was performed by tightening the prosthetic screw on the left molar abutment (terminal location) and right canine by using a hand screwdriver (Nobel Biocare AG).<sup>3,5,15,16</sup> After further tightening of the prosthetic screw to 15 Ncm at the terminal location (TL) with a calibrated torque wrench (Manual Torque Wrench-Prosthetic; Nobel Biocare AG), the screw on the right canine was unscrewed, and the 3D marginal discrepancy of frameworks was evaluated by using an

industrial metrology-grade CT scanner (XT H 225; Nikon Corp) and a 3D volumetric software program (PolyWorks - Modeler; InnovMetric Software Inc). The power settings of the CT scanner were adjusted for each material type scanned (PMMA versus Ti; Table 1). Because the voxel size is related to where the framework is in relation to the X-ray source and the detector, both PMMA and Ti frameworks positions were standardized during scanning by fixing the model with a clamp. Marginal gaps were measured by using planes created from scan data of the mating surfaces at the abutment-framework interface of the left canine (abutment #2), right canine (abutment #3), and right first molar (abutment #4) locations. Marginal discrepancy at the TL (location #1) was ignored because there was a screw and the STL bridging took place when the gap was not large enough to distinguish. Planes were fitted to the data by using a maximum-fit algorithm. The marginal gap was evaluated by using the standard method for measuring a distance between 2 planes and involved the use of a reference plane. The measurement was made by creating a line normal to the reference plane surface. This line was made to begin at the reference plane and end at the centroid of the other plane being considered. The 3D marginal discrepancy reported was the length of this line. The fixture surfaces were considered as the reference plane in this study (Fig. 1). Each framework was also scanned by an industrial metrology grade structured-light scanner (ATOS Compact Scan 5M; GOM GmbH) when it was secured on the model (key scan, 1 screw protocol). Then, the framework was removed from the model, and its occlusal and gingival surfaces were separately scanned. A pre-alignment and final alignment of the framework's occlusal and gingival scans were done by using a best-fit algorithm (GOM inspect V8 SR1; GOM GmbH). The alignment process generated a complete single framework scan (merged framework scan). Then, the model itself was also scanned to process the triple-scan protocol (Fig. 2) for 3D marginal gap measurements at abutment #2, abutment #3, and abutment #4.<sup>9</sup> For superimpositions, the model scan and the key scan were imported to a metrology software program (GOM inspect V8 SR1; GOM GmbH), and the model scan's coordinate system was selected as the basis. The areas other than the framework were then selected for superimpositions to avoid errors that may have occurred because of deviations of the scanned framework during alignment. A prealignment process for the scans was performed followed by a best-fit algorithm. The merged framework scan was imported along with the key scan into the model scan to bring all scans into a single-coordinate system. Then, the pre-alignment was performed for the merged framework scan and the key scan, followed by their final alignment. Because all scans were transferred to the same

**Table 1.** Settings for industrial computed tomography (CT) scanner when different frameworks scanned

Property	PMMA Framework	Ti Framework
Voxel size (mm)	0.04998	0.04998
X-ray kV	200	210
X-ray $\mu$ A	250	241

$\mu$ A, microampere; kV, kilovolt; PMMA, polymethylmethacrylate; Ti, titanium.

coordinate system, the scan file of the framework and the master model were determined to be properly superimposed and ready for gap measurements.

During structured-light scanner scans, the camera position was set at a small object to maximize the concentration of the pixels of the scanner's camera to a smaller volume, as the smaller the volume, the better the resolution according to the manufacturer. The measurement volume was 70×50×50 mm. To measure the gaps between the merged frame scan and the master model scan at the abutment-framework interface, 4 sectional cuts were made from an occlusal perspective at abutment positions 2, 3, and 4. Eight different views were used for gap measurements, and the gaps were averaged at each abutment site by using a software program (3Shape 3D Viewer; 3Shape AG). The position of the section cuts was standardized by using the identical section for each scan for each material (Fig. 2). Because the basis of the alignment was always the same master model scan, all merged framework scans could be superimposed in the same coordinate system, and the section cut locations could therefore be standardized.

The mean 3D marginal gap values for both PMMA and Ti frameworks from each industrial-grade scanner (structured-light versus CT) were calculated for each location (abutments 2, 3, and 4) and overall. The linear regression model was used to test the effects of material and scanner on the marginal gaps at each abutment site separately. To account for the heterogeneity of variance in the material-scanner subgroups, the weighted least squares value was used, and the weight was determined as the inverse of the estimated variance in each subgroup. The difference among gaps at 3 sites was also tested by the weighted linear regression in each material-scanner subgroup. Precision was analyzed with F-statistics. Specifically, the precision for each material-scanner subgroup was quantified by the inverse of variance of the marginal gap measures; the ratio of precision for each pair of subgroups was calculated, and then an F-test was performed to evaluate whether their precisions were significantly different. A Bonferroni correction was used to account for the comparison of pairs ( $\alpha=.05$ ). The sample size ( $n=5$ ) was not formally calculated but based on previously performed studies that used the same experiment design, test model, and CT scanner.<sup>3-5</sup>

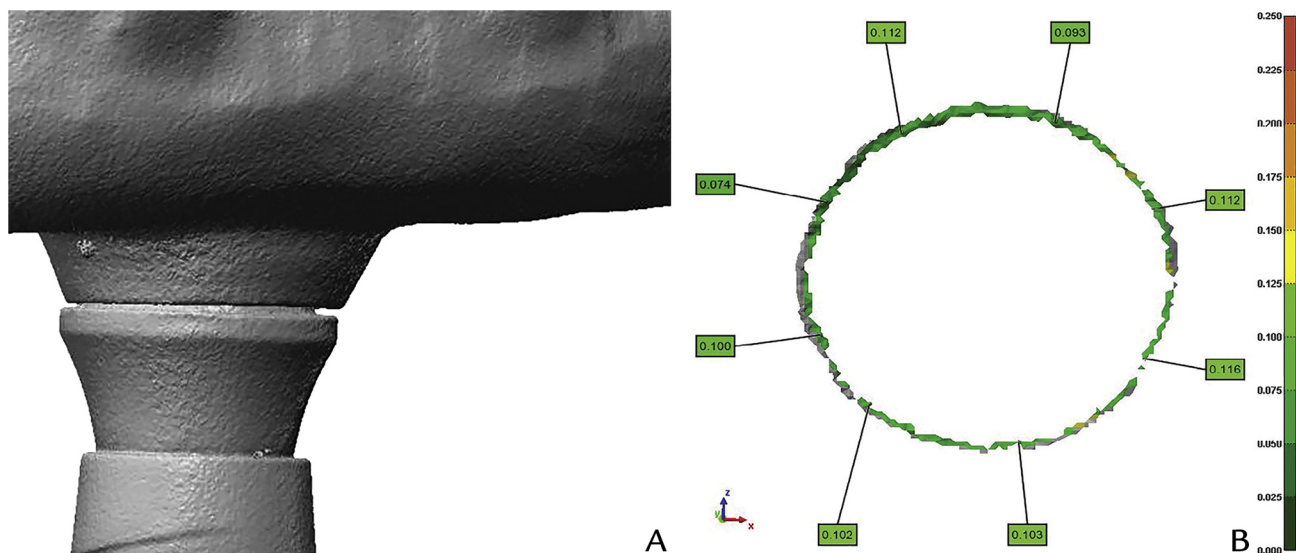


**Figure 1.** Gap measurements with CT scanner. A, CT scan at abutment-framework interface. B, Corresponding measurements of distance between mating surfaces with color map range up to +0.250 mm. CT, computed tomography.

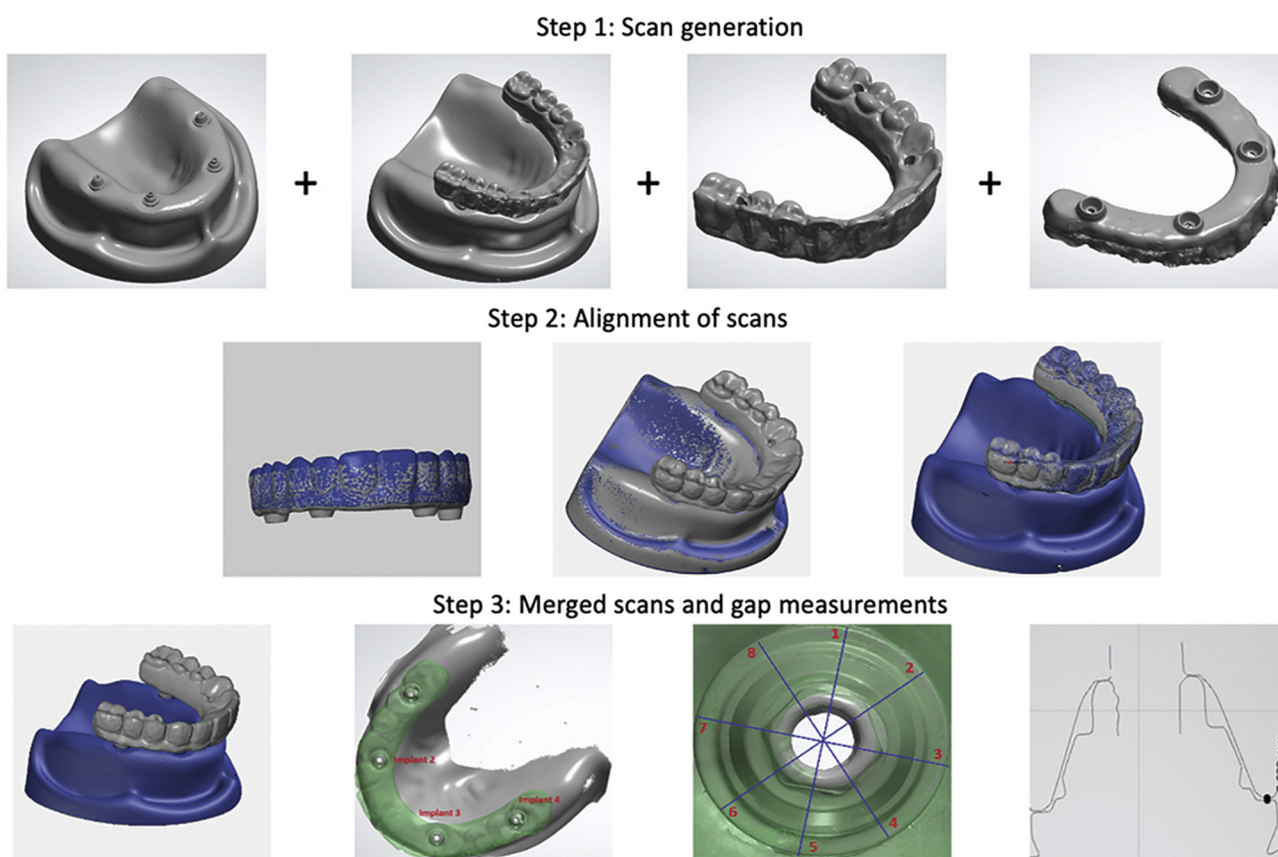


**Figure 2.** Triple-scan protocol and marginal gap measurement. Overview of triple-scan protocol (step 1 and 2), resulting merged scans, and gap measurement (step 3).

## RESULTS

When marginal gaps at different abutments were separately analyzed, the scanner, material, or their interaction

had no significant effect on the measured gaps on abutments 2 and 3 ( $P > .05$ ). For abutment 4, the interaction between the material and scanner was significant ( $P = .032$ ) (Table 2). When further resolved, a significant



**Table 2.** ANOVA table for abutment 4

Comparisons	Estimate	Std. Error	t Value	P
Material: Ti vs PMMA	0.026	0.012	2.104	.052
Scanner: Structured-light vs CT	-0.014	0.012	-1.202	.247
Interaction material:Scanner	-0.040	0.017	-2.347	.032

CT, computed tomography; PMMA, polymethylmethacrylate; Ti, titanium.

difference between the 2 scanners was found at abutment 4 with titanium frameworks ( $P=.003$ ). Gaps detected by using the CT scanner were greater than those detected by using the structured-light scanner (estimated difference in mean values=0.054 mm) (Table 3). For PMMA frameworks, the gaps detected by using both scanners were not significantly different (Fig. 3). When overall mean gap values, including all abutment sites in each material-scanner group, were considered, a significant difference was found between the scanners for titanium frameworks, and the gaps detected by using the CT scanner were significantly higher ( $P=.032$ ) (Fig. 4). When the difference among 3 abutment sites for each scanner-material subgroup was analyzed, no significant differences were found ( $P>.05$ ). The precision of the CT scanner was lower than that of the structured-light scanner when Ti frameworks were scanned ( $P=.001$ ). The CT scanner's precision was higher when scanning PMMA frameworks than when scanning Ti frameworks ( $P=.03$ ) (Figs. 3, 4).

## DISCUSSION

The first null hypothesis was rejected because the overall marginal gaps of the Ti frameworks and the gaps at abutment 4 as measured by using the CT scanner were significantly different from those measured by using the structured-light scanner. The second null hypothesis was also rejected as the precision of scanners was different and was affected by the material scanned.

Disadvantages of structured-light scanners include light reflection and scattering during scanning, inaccurate scans when undercuts are present, and the transformation of the point cloud to a common data format such as an STL file, all of which may compromise accuracy.<sup>17</sup> Furthermore, structured-light scanners may not be able to detect the small gaps between mating parts, especially when the gaps are smaller than the resolution of the scanner, defined as the closest distance of points that the scanner can discriminate.<sup>2-17</sup> In the present study, an industrial metrology-grade structured-light scanner, its software program, and the triple-scan technique were used to overcome these disadvantages. The scanner and the technique used should have enabled the highest possible accuracy with optical scans.<sup>18,19</sup> However, the arrangement of structured light in the present study may still not be conducive to a good line of sight given the intimate contact of the framework and the

**Table 3.** Difference between mean values (mm) measured with scanners (structured-light versus CT) and in linear regression models

Abutment	PMMA	Titanium
Overall	-0.009 ( $P=.18$ )	-0.023 ( $P=.033$ )
Abutment 2	-0.007 ( $P=.536$ )	0.001 ( $P=.969$ )
Abutment 3	-0.008 ( $P=.521$ )	-0.015 ( $P=.449$ )
Abutment 4	-0.014 ( $P=.264$ )	-0.054 ( $P=.003$ )

CT, computed tomography; PMMA, polymethylmethacrylate; Ti, titanium.

multiunit abutments. Accordingly, the structured-light scanner used may have been unable to provide complete data of the scanned area, especially when reflective titanium was scanned. The scanned material has been reported to affect the accuracy of structured-light scanners.<sup>12</sup> This may explain the smaller mean gaps and standard deviations detected by using the structured-light scanner than those detected when the titanium frameworks were scanned by using the CT scanner.

Industrial metrology-grade CT scanners have fewer line of sight concerns than structured-light scanners and are able to penetrate the inner areas of the abutment-framework interface, inaccessible with structured light. However, the radiation used contraindicates the clinical applicability of industrial CT scanners. In addition, the power settings used to scan objects with CT scanners affect the scan outcomes. The kV and  $\mu\text{A}$  are the basic settings to determine the power and are adjusted based on the material being scanned.<sup>20</sup> For the power to CT scan components, the kV and  $\mu\text{A}$  (power=voltage $\times$ amperes) settings are adjusted to produce the best possible image.<sup>20</sup> Therefore, the settings vary depending on the relative densities of the components to be scanned.<sup>21</sup> Among other considerations, when setting the CT scanner, adequate power should be balanced.<sup>22</sup> Prevention of excessive X-ray energy is essential so that the image is not washed out.<sup>2</sup> Although X-rays can penetrate the interface and image the marginal gaps with high accuracy ( $\pm 10 \mu\text{m}$ ),<sup>5</sup> metal components can compromise the accuracy of the analysis by causing scatter and artifacts.<sup>23</sup> The deeper penetration of the X-rays into the interface in combination with scatter and artifacts may be why the higher standard deviations (lower precision) with the CT scans compared with the structured-light scans of Ti frameworks in the present study. Accordingly, CT scanners might be less suitable for analyzing the gaps between metal components. However, the CT scanner performed similarly to the structured-light scanner when detecting the gaps in PMMA and can be recommended for the marginal gap analysis of polymer frameworks.

The voxel size of CT scanners has been demonstrated as a factor for the accuracy of CT scan images and related measurements.<sup>24</sup> Small voxel sizes are associated with high accuracy<sup>25</sup>; the smaller the voxel, the higher the resolution of the data. Whether a gap between 2 parts

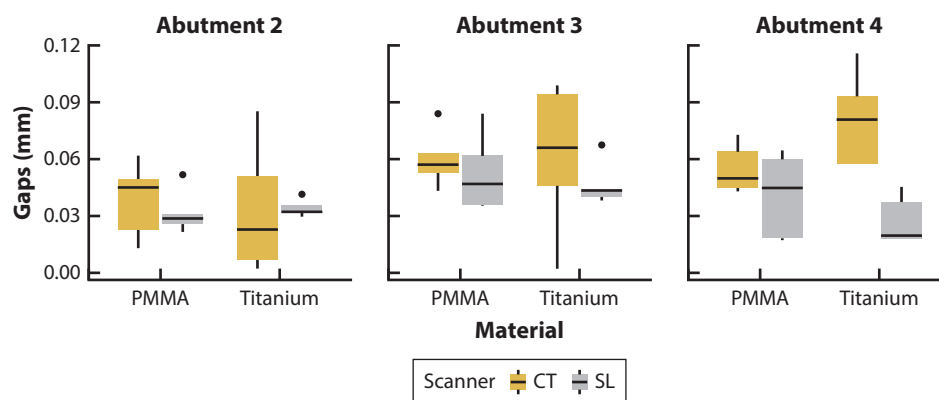


**Figure 3.** Box plot for effect of material and scanner on gap values at each abutment site. CT, computed tomography; PMMA, polymethylmethacrylate; SL, structured light.

closer than 1 voxel in size is measurable is unclear, although it may be measurable with subvoxel surface determination and by determining the number of voxels involved and continuous surfaces. Each voxel is cube-shaped and therefore has an edge length and an associated grayscale value<sup>26</sup> that can help determine whether that area is air, a particular material, or a piece of a particular material.<sup>27</sup> The software program makes reasonable assumptions about continuous surfaces, and because real surfaces do not have discontinuities, the software program uses this fact in surface determination.<sup>28</sup> Combining those assumptions and information from the surrounding voxels, subvoxel size gaps can be captured. The measurement uncertainty of the CT scanner used in the present study was approximately  $8 + 0.29L \mu\text{m}$  with a 95% confidence interval, allowing the accurate capture of surfaces within this value, where  $L$  represents the length of the object scanned in meters. The largest distance in the frameworks analyzed in the present study was 56 mm, making the highest uncertainty 12.59  $\mu\text{m}$ .

Different digital methods have been used to evaluate gaps by using different algorithms, including the commonly used best-fit algorithm.<sup>2-29</sup> In the triple-scan technique, the alignment process is essential for the accuracy of assessment. Good alignment accurately duplicates the relative position of the intaglio surface to the abutment.<sup>30</sup> However, because most algorithms, including the best-fit algorithm, overlay the 3D data sets without completely simulating actual physical contacts, such techniques must be executed with caution.<sup>9</sup> Because the algorithm attempts to superimpose 2 corresponding surface scans with the minimum difference between all surface points, the real distances between selected points may be underestimated.<sup>12</sup> When such an algorithm is used, the fitted plane may intersect some of the part data, not representative of part functionality because mating surfaces do not intersect when in contact with one

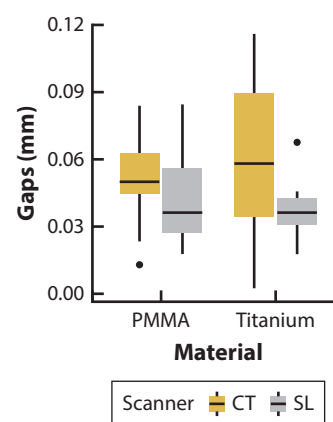


**Figure 4.** Box plot for overall effect of material and scanner on gap values. CT, computed tomography; PMMA, polymethylmethacrylate; SL, structured light.

another. This intersection results in an underestimation of the marginal gaps.<sup>31</sup> The maximum-fit algorithm, as used with the CT scanner system in the present study, uses a tripod contact between the framework and the master model to create a plane, matching the physical situation more accurately.<sup>28</sup> The algorithm fits a plane to only the highest eligible data points. The CT software program enables the use of billions of data points when averaging the circumferential marginal gap value. However, data from the triple scan are limited to the section cuts selected.

The marginal gap values for all frameworks can be considered suitable for the fabrication of prosthetic frameworks with the applied CAD-CAM system. The maximum marginal gap was below 150  $\mu\text{m}$  at each implant position, which has been described as a clinically acceptable value.<sup>5</sup> The marginal gaps in the present study are comparable with those measured on the same model in previous studies when different materials were tested.<sup>3-5</sup>

The present study had a small sample size, and only 2 framework materials were tested. The number of specimens was determined by considering previous studies which used an identical experiment design, test model, and CT scanner and were able to detect and report statistical differences.<sup>3-5</sup> The fact that highly significant differences were detected shows the adequate power of the statistical and experimental design in the present study. The materials tested were selected because of their common use in dentistry and their surface and inner properties; Ti has increased potential for reflection and scattering compared with PMMA and therefore an increased interaction between the material and the scanners. Future studies should also investigate zirconia frameworks.

Optical laboratory scanners and microCTs have been used in previous studies to obtain reference scans and for marginal gap measurements.<sup>2,32,33</sup> However, microCT scanners are not suitable for use with larger frameworks.<sup>34</sup> In addition, industrial scanners have higher accuracy than dental laboratory scanners.<sup>2</sup> Photogrammetry has also been used to measure gaps between implant abutments and frameworks but provides lower accuracy compared with other methods.<sup>35</sup> Another metrology-grade option, a coordinate measuring machine (CMM), has probes that enable surface detection in detail with a precision of  $\pm 1 \mu\text{m}$ .<sup>36</sup> However, most of the CMM probes are larger than potential gaps at the framework-abutment interface. Therefore, direct measurement of the gaps with a CMM is not feasible.<sup>35</sup> CMMs may be used for indirect gap measurements by scanning the mating surfaces separately and then transferring them to a coordinate system.<sup>35,36</sup> However, a CMM was not available to the authors during the present study.

## CONCLUSIONS

Based on the findings of this in vitro study, the following conclusions were drawn:

1. The measured marginal gaps depended on the material and abutment location.
2. The overall measured marginal gaps of the titanium framework varied in the scans from the 2 scanners and also in the scan at the abutment most distant from the tightened prosthetic screw.
3. The structured-light scanner may be preferred over the CT scanner for the evaluation of gaps at titanium-titanium interfaces because of the lower precision observed with the Ti framework scans from the CT scanner. However, the Ti framework scans from the structured-light scanner may also lead to an underestimation of the discrepancy, as the detected gaps were smaller than those with the CT scanner.

## REFERENCES

1. Janda M, Larsson C, Mattheos N. Influence of misfit on the occurrence of porcelain veneer fractures in implant-supported metal-ceramic fixed dental prostheses. Part 2: a three-dimensional finite element analysis. *Int J Prosthodont* 2021;34:458-62.
2. Pan Y, Tsoi JKH, Lam WYH, Pow EHN. Implant framework misfit: a systematic review on assessment methods and clinical complications. *Clin Implant Dent Relat Res* 2021;23:244-58.
3. Yilmaz B, Alshahrani FA, Kale E, Johnston WM. Effect of feldspathic porcelain layering on the marginal fit of zirconia and titanium complete-arch fixed implant-supported frameworks. *J Prosthet Dent* 2018;120:71-8.
4. Yilmaz B, Kale E, Johnston WM. Marginal discrepancy of CAD-CAM complete-arch fixed implant-supported frameworks. *J Prosthet Dent* 2018;120:65-70.
5. AL-Meraikhi H, Yilmaz B, McClumphy E, Brantley W, Johnston WM. In vitro fit of CAD-CAM complete arch screw-retained titanium and zirconia implant prostheses fabricated on 4 implants. *J Prosthet Dent* 2018;119:409-16.
6. Boitelle P, Tapie L, Mawussi B, Fromentin O. Evaluation of the marginal fit of CAD-CAM zirconia copings: comparison of 2D and 3D measurement methods. *J Prosthet Dent* 2018;119:75-81.
7. Li R, Chen H, Wang Y, Sun Y. Suitability of the triple-scan method with a dental laboratory scanner to assess the 3D adaptation of zirconia crowns. *J Prosthet Dent* 2021;125:651-6.
8. Maeng YJ, Lee HS, Lee ES, Yoon HC, Kim BI. Noninvasive detection of microleakage in all-ceramic crowns using quantitative light-induced fluorescence technology. *Photodiagnosis Photodyn Ther* 2020;30:101672.
9. Holst S, Karl M, Wichmann M, Matta RE. A new triple-scan protocol for 3D fit assessment of dental restorations. *Quintessence Int* 2011;42:651-7.
10. Holst S, Karl M, Wichmann M, Matta RE. A technique for in vitro fit assessment of multi-unit screw-retained implant restorations: application of a triple-scan protocol. *J Dent Biomech* 2012;3:1-7.
11. Kim M, Kim J, Mai HN, Kwon TY, Choi Y-D, Lee CH, et al. Comparative clinical study of the marginal discrepancy of fixed dental prosthesis fabricated by the milling-sintering method using a presintered alloy. *J Adv Prosthodont* 2019;11:280-5.
12. O'Toole S, Osnes C, Bartlett D, Keeling A. Investigation into the accuracy and measurement methods of sequential 3D dental scan alignment. *Dent Mater* 2019;35:495-500.
13. Hategan SI, Ionel TF, Goguta L, Gavrilovici A, Negrutiu ML, Jivanescu A. Powder and powder-free intra-oral scanners: digital impression accuracy. *Prim Dent J* 2018;7:40-3.
14. Dutton E, Ludlow M, Mennito A, Kelly A, Evans Z, Culp A, et al. The effect different substrates have on the trueness and precision of eight different intraoral scanners. *J Esthet Restor Dent* 2020;32:204-18.
15. Yilmaz B. CAD-CAM high-density polymer implant-supported fixed diagnostic prostheses. *J Prosthet Dent* 2018;119:688-92.
16. Ercoli C, Geminiani A, Feng C, Lee H. The influence of verification jig on framework fit for nonsegmented fixed implant-supported complete denture. *Clin Implant Dent Relat Res* 2012;14 Suppl 1:e188-95.
17. Vlaar ST, Van Der Zel JM. Accuracy of dental digitizers. *Int Dent J* 2006;56:301-9.
18. Çakmak G, Yilmaz H, Treviño A, Kökat AM, Yilmaz B. The effect of scanner type and scan body position on the accuracy of complete-arch digital implant scans. *Clin Implant Dent Relat Res* 2020;22:533-41.
19. Schimmel M, Akino N, Srinivasan M, Wittneben JG, Yilmaz B, Abou-Ayash S. Accuracy of intraoral scanning in completely and partially edentulous maxillary and mandibular jaws: an in vitro analysis. *Clin Oral Investig* 2021;25:1839-47.
20. Eloeimy S, Tipnis S, Huda W. Relationship between radiographic techniques (kilovolt and milliampere-second) and CT DIvol. *Radiat Prot Dosimetry* 2010;141:43-9.
21. Omami G. Cone-beam computed tomography in implant dentistry: back to the future. *J Oral Maxillofac Surg* 2017;75:655.
22. Huda W, Ogden KM, Khorasani MR. Effect of dose metrics and radiation risk models when optimizing CT x-ray tube voltage. *Phys Med Biol* 2008;53:4719-32.
23. Schriber M, Yeung AWK, Suter VGA, Buser D, Leung YY, Bornstein MM. Cone beam computed tomography artefacts around dental implants with different materials influencing the detection of peri-implant bone defects. *Clin Oral Implants Res* 2020;31:595-606.
24. Maret D, Peters OA, Galibourg A, Dumoncel J, Esclassan R, Kahn JL, et al. Comparison of the accuracy of 3-dimensional cone-beam computed tomography and micro-computed tomography reconstructions by using different voxel sizes. *J Endod* 2014;40:1321-6.
25. Tjong W, Kazakia GJ, Burghardt AJ, Majumdar S. The effect of voxel size on high-resolution peripheral computed tomography measurements of trabecular and cortical bone microstructure. *Med Phys* 2012;39:1893-903.
26. Shafiq-Ul-Hassan M, Zhang GG, Latifi K, Ullah G, Hunt DC, Balagurunathan Y, et al. Intrinsic dependencies of CT radiomic features on voxel size and number of gray levels. *Med Phys* 2017;44:1050-62.

27. Mullan BF, Galvin JR, Zabner J, Hoffman EA. Evaluation of in vivo total and regional air content and distribution in primate lungs with high-resolution CT. *Acad Radiol* 1997;4:674-9.
28. Blazejewska AL, Fischl B, Wald LL, Polimeni JR. Intracortical smoothing of small-voxel fMRI data can provide increased detection power without spatial resolution losses compared to conventional large-voxel fMRI data. *Neuroimage* 2019;189:601-14.
29. Hjalmarsson L, Örtorp A, Smedberg JL, Jemt T. Precision of fit to implants: a comparison of Cresco™ and Procera® implant bridge frameworks. *Clin Implant Dent Relat Res* 2010;12:271-80.
30. Kirschneck C, Kamuf B, Putsch C, Chhatwani S, Bizhang M, Danesh G. Conformity, reliability and validity of digital dental models created by clinical intraoral scanning and extraoral plaster model digitization workflows. *Comput Biol Med* 2018;100:114-22.
31. Jemt T, Hjalmarsson L. In vitro measurements of precision of fit of implant-supported frameworks. A comparison between "virtual" and "physical" assessments of fit using two different techniques of measurements. *Clin Implant Dent Relat Res* 2012;14 Suppl 1:e175-82.
32. González de Villambrosia P, Martínez-Rus F, García-Orejas A, Salido MP, Pradies G. In vitro comparison of the accuracy (trueness and precision) of six extraoral dental scanners with different scanning technologies. *J Prosthet Dent* 2016;116:543-50.e1.
33. Moris ICM, Monteiro SB, Martins R, Ribeiro RF, Gomes EA. Influence of manufacturing methods of implant-supported crowns on external and internal marginal fit: a micro-CT analysis. *Biomed Res Int* 2018;2018:5049605.
34. Yu H, Li L, Tan C, Liu F, Zhou R. X-ray source translation based computed tomography (STCT). *Opt Express* 2021;29:19743-58.
35. Jemt T, Rubenstein JE, Carlsson L, Lang BR. Measuring fit at the implant prosthodontic interface. *J Prosthet Dent* 1996;75:314-25.
36. Revilla-León M, Sánchez-Rubio JL, Pérez-López J, Rubenstein J, Özcan M. Discrepancy at the implant abutment-prosthesis interface of complete-arch cobalt-chromium implant frameworks fabricated by additive and subtractive technologies before and after ceramic veneering. *J Prosthet Dent* 2021;125:795-803.

**Corresponding author:**

Dr Samir Abou-Ayash  
Department of Reconstructive Dentistry and Gerodontology  
University of Bern  
Bern  
SWITZERLAND  
Email: Samir.abou-ayash@zmk.unibe.ch

**Acknowledgments**

The authors thank Drs Hadi Al-Meraikhi, Ediz Kale, and Hakan Yilmaz for their support in experiments and manuscript preparation; Mr Rob Glassburn at 3D Engineering Solutions for his expertise in interpretation of CT scanner data, and Mr Ralph Erhard at NT-Trading for his support in superimpositions and measurements.

Copyright © 2021 by the The Authors. This is an open access article under the CC BY-NC-ND license (<http://creativecommons.org/licenses/by-nc-nd/4.0/>).  
<https://doi.org/10.1016/j.prosdent.2021.10.013>